



## Nitric oxide delivery by ultrasonic cracking: some limitations

Michiel Postema, Ayache Bouakaz, Folkert J. ten Cate, Georg Schmitz, Nico de Jong, Annemieke van Wamel

### ► To cite this version:

Michiel Postema, Ayache Bouakaz, Folkert J. ten Cate, Georg Schmitz, Nico de Jong, et al.. Nitric oxide delivery by ultrasonic cracking: some limitations. *Ultrasonics*, 2006, Proceedings of Ultrasonics International (UI'05) and World Congress on Ultrasonics (WCU), 29 August-1 September 2005, Beijing, China, 44 (Suppl.), pp.e109-e113. 10.1016/j.ultras.2006.06.003 . hal-03193334

**HAL Id: hal-03193334**

**<https://hal.science/hal-03193334>**

Submitted on 11 Apr 2021

**HAL** is a multi-disciplinary open access archive for the deposit and dissemination of scientific research documents, whether they are published or not. The documents may come from teaching and research institutions in France or abroad, or from public or private research centers.

L'archive ouverte pluridisciplinaire **HAL**, est destinée au dépôt et à la diffusion de documents scientifiques de niveau recherche, publiés ou non, émanant des établissements d'enseignement et de recherche français ou étrangers, des laboratoires publics ou privés.



Distributed under a Creative Commons Attribution - NonCommercial - NoDerivatives 4.0 International License

## Nitric oxide delivery by ultrasonic cracking: some limitations

Michiel Postema<sup>1</sup>, Ayache Bouakaz<sup>2</sup>, Folkert J. ten Cate<sup>3</sup>, Georg Schmitz<sup>1</sup>, Nico de Jong<sup>4,5,6</sup>,

Annemieke van Wamel<sup>4,5</sup>

<sup>1</sup> Institute for Medical Engineering, Ruhr-Universität Bochum, Bochum, Germany;

<sup>2</sup> INSERM 619, Université François-Rabelais, Tours, France;

<sup>3</sup> Dept. of Cardiology, Thoraxcentre, Erasmus MC, Rotterdam, The Netherlands;

<sup>4</sup> Dept. of Biomedical Engineering, Thoraxcentre, Erasmus MC, Rotterdam, The Netherlands;

<sup>5</sup> Interuniversity Cardiology Institute of the Netherlands, Utrecht, The Netherlands;

<sup>6</sup> Physics of Fluids Group, Faculty of Science and Technology, University of Twente, Enschede, The Netherlands.

corresponding author:

Michiel Postema, MSc, PhD, Institute for Medical Engineering, Ruhr-Universität Bochum, Building IC, 6/146,  
D-44780 Bochum, Germany;

tel: +49 234 32 27740; E-mail: michiel.postema@ruhr-uni-bochum.de

Running title: Nitric oxide delivery

## Abstract

Nitric oxide (NO) has been implicated in smooth muscle relaxation. Its use has been widespread in cardiology. Due to the effective scavenging of NO by hemoglobin, however, the drug has to be applied locally or in large quantities, to have the effect desired. We propose the use of encapsulated microbubbles that act as a vehicle to carry the gas to a region of interest. By applying a burst of high-amplitude ultrasound, the shell encapsulating the gas can be cracked. Consequently, the gas is released upon which its dissolution and diffusion begins. This process is generally referred to as (ultra)sonic cracking.

To test if the quantities of released gas are high enough to allow for NO-delivery in small vessels ( $\varnothing < 200 \mu\text{m}$ ), we analyzed high-speed optical recordings of insonified stiff-shelled microbubbles. These microbubbles were subjected to ultrasonic cracking using 0.5 or 1.7 MHz ultrasound with mechanical index  $MI > 0.6$ . The mean quantity released from a single microbubble is 1.7 femtomol. This is already more than the NO production of a 1 mm long vessel with a  $50 \mu\text{m}$  diameter during 100 ms. However, we simulated that the dissolution time

of typical released NO microbubbles is equal to the half-life time of NO in whole blood due to scavenging by hemoglobin (1.8 ms), but much smaller than the extravascular half-life time of NO (>90 ms).

We conclude that ultrasonic cracking can only be a successful means for nitric oxide delivery, if the gas is released in or near the red blood cell-free plasma next to the endothelium. A complicating factor in the *in vivo* situation is the variation in blood pressure. Although our simulations and acoustic measurements demonstrate that the dissolution speed of free gas increases with the hydrostatic pressure, the *in vitro* acoustic amplitudes suggest that the number of released microbubbles decreases at higher hydrostatic pressures. This indicates that ultrasonic cracking mostly occurs during the expansion phase.

## 1 Introduction

In 1992, the radical nitric oxide (NO) was declared molecule of the year [1]. Since then, increased scientific interest has been shown in its therapeutic applications. NO is one of the 10 smallest, stable molecules of the hundreds of millions in nature [2]. The complexity of the biological processes involving NO is in contrast to the simplicity of its molecular structure [3]. In the vasculature (*cf.* Fig. 1), NO is produced by the endothelium and diffuses into the luminal and abluminal regions. The steady-state tissue concentration lies between 10 nM and 1  $\mu$ M [4]. The average NO production by the endothelium has been estimated  $6.8 \times 10^{-14} \mu\text{mol} \mu\text{m}^{-2} \text{s}^{-1}$  [5]. NO traveling into smooth muscle initiates a series of reactions that lead to vessel dilation [5]. In the lumen, NO is consumed by the nearly irreversible reaction with hemoglobin within the erythrocytes. Because of this so-called scavenging, the half-life of NO in the lumen is only 1.8 ms [2], whereas the extravascular half-life of NO has been determined to be more than 90 ms [6]. The blood in the vicinity of the endothelium contains little or no erythrocytes. This thin plasma layer has been estimated between 2.6% and 12.5% of the lumen diameter [7]. NO molecules in this layer are not scavenged by erythrocytes. The consumption rate of NO has been noted to be lower in smaller vessels [8], although the plasma layers in smaller vessels are relatively thinner.

In clinical cardiology, NO finds applications in post-myocardial infarction treatment. Targeting NO to areas of early atherosclerosis might prove useful in preventing plaque formation [9]. Due to the high diffusivity of NO, however, the drug has to be applied locally or in large quantities, in order to have the effect desired. Here, ultrasound-induced bubble-assisted drug delivery may prove to be fruitful. Small quantities of NO might be administered, and released at the region of interest by means of high-amplitude ultrasound. This technique has been referred to as (ultra)sonic cracking [10].

Other microbubble-based delivery methods proposed involve mixing microbubbles with therapeutic agents

[11], attaching a drug or gene to the shell [12], incorporating an oil layer inside the shell with a drug dissolved in it [13], or including therapeutic agents in antibubbles [14].

To test if the quantities of released gas are high enough to allow for NO-delivery in small vessels ( $\varnothing < 200 \mu\text{m}$ ), we analyzed high-speed optical and acoustical recordings of stiff-shelled microbubbles.

## 2 Theory

Ultrasound contrast agents have been applied in clinical diagnostics, mostly for perfusion imaging. They consist of gas microbubbles encapsulated by an elastic shell. The shell withholds the gas from dissolving, at least until it has reached a target area. Because the shell has to be biodegradable, albumins and lipids are its preferred compounds. Especially microbubbles with a stiff shell demonstrate oscillation amplitudes much lower than those of free gas bubbles of the same size. Therefore, much less sound is scattered from stiff-shelled agents than from free gas bubbles. However, when stiff-shelled microbubbles are subjected to an ultrasound field, the gas content may be forced out, which increases the acoustic scattering dramatically. The quasiisostatic pressures at which such shells rupture have been under investigation. They lie in the range 0.1–1 MPa [15]. If the driving frequency of an ultrasonic burst is much lower than the resonance frequency of the microbubbles, the pressure field may be considered quasiisostatic.

The cracking of materials may take place during rarefaction or compression [16]. Stiff, thick shells of microbubbles may crack during microbubble expansion or contraction. During rarefaction, the liquid pressure outside such a bubble  $p_L$  is decreased with respect to the pressure  $p_g$  inside the bubble, resulting in bubble expansion [17]. During compression,  $p_L$  is increased with respect to  $p_g$ , resulting in bubble contraction. Hence, the critical expansion or contraction at which a shell cracks corresponds to a critical pressure difference  $\Delta p_c$  between the inside and the outside of the bubble. For small radial changes,  $p_g$  may be considered constant. For encapsulated microbubbles insonified below their resonance frequency, the expansion phase corresponds to the rarefaction phase of the ultrasonic cycle, and the contraction phase to the compression phase of the ultrasonic cycle [18]. Here, the liquid pressure is a periodic function  $p_L(t) = p_a \sin \omega t + p_0$ , where  $p_0$  is the ambient pressure,  $p_a$  is the acoustic amplitude, and  $\omega$  is the insonifying frequency. Clearly, introducing a hydrostatic overpressure  $p^+$  will give  $p_L^+(t) = p_a \sin \omega t + p^+ + p_0$ . If ultrasonic cracking takes place during the expansion of the shell ( $\Delta p_c < 0$ ), introducing a hydrostatic overpressure will decrease the cracking rate, because  $p_g - p_L^+(\omega t = -\frac{1}{2}\pi) = p_g - (-p_a + p^+ + p_0) < p_g - (-p_a + p_0) = p_g - p_L(\omega t = -\frac{1}{2}\pi)$ . If ultrasonic cracking of stiff-shelled microbubbles takes place during the contraction of the shell ( $\Delta p_c > 0$ ), introducing a hydrostatic overpressure will increase

the cracking rate, because  $p_L^+(\omega t = \frac{1}{2}\pi) - p_g = (p_a + p^+ + p_0) - p_g > (p_a + p_0) - p_g = p_L(\omega t = \frac{1}{2}\pi) - p_g$ .

After cracking of the shell, the gas content may be set free. Owing to the rarefaction phase of the ultrasound, the pressure difference between the inside of the microbubble and the surrounding fluid will force (part of) the gas out of the shell (*cf.* Figure 2). This gas escape continues until the compression phase of the ultrasonic wave causes the free gas to contract. During contraction, the released gas detaches from the shell. Optical observations have demonstrated that some gas remains within the shell, so that the cracked microbubble stays acoustically active [19].

The process of ultrasonic cracking and gas release occurs within one ultrasonic cycle. The subsequent dissolution of the released gas bubble takes much longer. It is given by the following differential equation [20, 19]:

$$\frac{dR}{dt} = DL \left( \frac{\frac{C_i}{C_0} - 1 - \frac{2\sigma}{R p_0} - \frac{p_{ov}}{p_0}}{1 + \frac{4\sigma}{3 R p_0}} \right) \left( \frac{1}{R} + \frac{1}{\sqrt{\pi D t}} \right), \quad (1)$$

where  $\frac{C_i}{C_0}$  is the ratio of the dissolved gas concentration to the saturation concentration (saturation ratio),  $D$  is the diffusion constant,  $L$  is the Ostwald coefficient,  $p_0$  is the ambient pressure,  $p_{ov}$  is the applied overpressure,  $R$  is the instantaneous bubble radius,  $t$  is the time starting ( $t = 0$ ) when the bubble surface is exposed to the liquid surface, and  $\sigma$  is the surface tension. Equation (1) shows that the disappearance of gas bubbles in a liquid medium is highly influenced by gas diffusion parameters and applied overpressure, and that the disappearance time of gas bubbles is shorter when the liquid medium is under pressure.

The mean traveled distance of the dissolved molecules can be computed with [21]:

$$\langle r^2 \rangle = 6 D t. \quad (2)$$

### 3 Methods

To illustrate the rapid dissolution of NO at 0 and 100 mmHg overpressure, equation (1) was solved numerically, using a MATLAB<sup>®</sup> (The MathWorks, Inc., Natick, MA) program. The parameters used have been summarized in Table 1.

For the observations of ultrasonic cracking, we made use of fast framing camera systems, taking two-dimensional frames at 3 MHz and up during ultrasonic insonification. Ultrasound contrast agent microbubbles, freely flowing through a  $\varnothing < 200 \mu\text{m}$  cellulose artificial vessel, were subjected to 0.5 or 1.7 MHz ultrasound with mechanical index  $MI > 0.6$ . The contrast agents used were PB127 (POINT Biomedical

Corporation, San Carlos, CA) and Quantison<sup>TM</sup> (Upperton Limited, Nottingham, UK). In all optical observations, several frames were taken during ultrasound insonification.

To investigate the influence of realistic *in vivo* blood pressures on the cracking rate, we performed 20 acoustic experiments in a sealed Perspex container of  $15 \times 15 \times 10 \text{ cm}^3$ . Two transducers were fixed in the middle of perpendicular sides of the container [20]. Both transducers were spherically focused at a distance of 7.5 cm. The transducers were so positioned, that the acoustic foci overlapped. The container was filled with saturated water. 30 mg of Quantison<sup>TM</sup> was stirred through the water. The isostatic pressure was controlled with a sphygmomanometer. In each event, a burst of 10 cycles of 0.5 MHz ultrasound was transmitted at  $MI > 0.6$ , to release gas from the shells. With a pulse repetition frequency  $> 1 \text{ kHz}$ , a burst of 5 cycles of 5 MHz ultrasound at  $MI < 0.1$  was transmitted and received, to record the release and the dissolution of the released gas. To increase the signal-to-noise ratio, the acoustic data corresponding to one hydrostatic overpressure were added.

## 4 Results and discussion

An overview of our optical observations of gas release from contrast agents has been separately presented in [19]. For both insonifying frequencies, the released gas microbubbles from PB127 have a mean diameter of  $1.5 \mu\text{m}$  [19]. The mean quantity released from a single microbubble is therefore 1.7 femtomol. This is already more than the average NO production of a 1 mm long vessel with a  $50 \mu\text{m}$  diameter during 100 ms. A limiting factor is the low cracking rate. At high MI, less than 40% of the microbubbles have been observed to crack during an 8-cycle burst [19]. This limitation can be overcome by applying multiple high-MI bursts: When applying multiple bursts on the same contrast agent sample, ‘fresh’ microbubbles have been observed to crack during subsequent bursts [19]. The microbubbles in our experiments were nitrogen- or air-filled. Using NO-filled microbubbles instead would not affect the cracking rate, provided that the physical conditions are kept constant, because the change in acoustic impedance is negligible.

Dissolution curves were computed at ambient pressure and at an overpressure of 100 mmHg. The results are shown in Figure 3 for diameters below  $2 \mu\text{m}$ . Nitric oxide bubbles dissolve much faster than air bubbles. In comparison, the half-size time of a free nitrogen microbubble with a  $6 \mu\text{m}$  diameter is 99 ms [22], whereas the half-size time of a nitric oxide microbubble of the same size is less than 25 ms. After applying a 100 mmHg overpressure, a speed-up of the dissolution can be observed, especially with bigger microbubbles. Still, according to equation (2) a dissolved NO molecule needs 5 ms to travel only  $10 \mu\text{m}$ , which is more than twice the intravascular half-life of NO. A solution may be found in the release of NO in or near the erythrocyte-free

plasma layer. Microbubbles with elastic shells may be targeted to the vessel wall with a continuous, low-MI ultrasonic wave-train that induces primary radiation forces, after which the content can be released with a high-MI burst [13]. In our case, the shells are so stiff, that the effects of radiation forces have not been observed. However, gas microbubbles that have been released in the lumen can also be targeted towards the endothelium by primary radiation forces [10]. Translation velocities on the order of  $1 \text{ m s}^{-1}$  can be reached, driving the NO bubbles into the plasma layer within a millisecond.

The results of the acoustic measurements of bubble dissolution after ultrasonic release are presented in Figure 4. Clearly, the acoustic amplitudes decrease more rapidly with increasing hydrostatic overpressure, as would be expected from equation (1). The measurements were done on bulk agent. Hence, the acoustic signal recorded was generated by numerous released bubbles with a variety of sizes. If we assume the same size distribution of release gas bubbles for different hydrostatic overpressures, we can investigate how the number of released gas bubbles depends on the hydrostatic overpressure applied. Figure 5 shows the peak of the positive acoustic response as a function of the hydrostatic overpressure applied. These peaks have been observed during gas release, caused by the quasiisostatic ultrasonic field with a center frequency of 0.5 MHz. Error bars were computed using a noise level of 1 mV. The peak response at 60 mmHg hydrostatic overpressure is 1.7 dB lower than at 0 mmHg, at 100 mmHg it is 3.4 dB lower, and at 200 mmHg it is 4.2 dB lower. The peak acoustic response from released gas microbubbles decreases with hydrostatic overpressure. This suggests that the number of released gas bubbles is lower, and that less contrast agent microbubbles crack during a high-MI burst. Hence, following our analysis on the influence of the hydrostatic overpressure on the cracking rate, most stiff-shelled microbubbles crack during the rarefaction phase.

In a saturated solution, the NO concentration is approximately 3 mM [4]. A vial of contrast agents contains up to  $10^9$  microbubbles. Even if all these microbubbles would crack and dissolve, assuming equal distribution throughout the human body, the NO concentration in the blood would still be less than  $\frac{1}{10}^{\text{th}}$  of the saturated solution concentration. Therefore, our assumption that the saturation ratio is approximately zero is justified. Clearly, the steady-state tissue concentration of NO can be neglected.

In the acoustic regime where sonic cracking occurs, the phenomenon of microbubble jetting has been observed [10]: microbubbles acting as microsyringes. This mechanism has been under investigation for therapeutic purposes. We observed the jetting phenomenon with released gas bubbles [23]. This may prove to be useful in NO delivery.

## 5 Conclusions

In clinical cardiology, NO finds applications in post-myocardial infarction treatment. Here, ultrasound-induced bubble-assisted NO delivery may prove to be helpful. Small quantities of NO might be administered, and released at the region of interest by means of high-amplitude ultrasound. Released gas may be targeted by means of primary radiation forces.

We conclude that ultrasonic cracking can only be a successful means for nitric oxide delivery, if the gas is released in or near the red blood-free plasma next to the endothelium.

When applying an isostatic overpressure, the response from the released gas microbubbles decreases, suggesting that the number of released microbubbles is smaller. It is concluded that ultrasonic cracking of stiff-shelled microbubbles mostly occurs during microbubbles expansion, rather than during contraction. Therefore, sonic cracking may be more effective during the diastolic phase of a cardiac cycle.

## Acknowledgments

The authors are grateful for the contrast agent PB127 supplied by POINT Biomedical Corporation, San Carlos, CA, and for the contrast agent Quantison<sup>TM</sup> supplied by Upperton Limited, Nottingham, UK.

## References

- [1] D. E. Koshland Jr., The molecule of the year, *Science* 258 (1992) 1861.
- [2] X. Liu, M. J. S. Miller, M. S. Joshi, H. Sadowska-Krowicka, D. A. Clark, J. R. Lancaster Jr., Diffusion-limited reaction of free nitric oxide with erythrocytes, *J. Biol. Chem.* 273 (30) (1998) 18709–18713.
- [3] M. Pfaffendorf, NO — the molecule, *Neth. J. Crit. Care* 6 (5) (2002) 7–11.
- [4] I. Bilic, Pathophysiological role of nitric oxide, *Prog. Rep. 1st Reg. Meet. HNE-Club* (2001) 8–9.
- [5] M. W. Vaughn, L. Kuo, J. C. Liao, Estimation of nitric oxide production and reaction rates in tissue by use of a mathematical model, *Am. J. Physiol.* 274 (1998) H2163–H2176.
- [6] D. D. Thomas, X. Liu, S. P. Kantrow, J. R. Lancaster Jr., The biological lifetime of nitric oxide: implications for the perivascular dynamics of NO and O<sub>2</sub>, *PNAS* 98 (1) (2001) 355–360.
- [7] A. R. Butler, I. L. Megson, P. G. Wright, Diffusion of nitric oxide and scavenging by blood in the vasculature, *Biochim. Biophys. Acta* 1425 (1998) 168–176.



- [8] M. W. Vaughn, L. Kuo, J. C. Liao, Effective diffusion of nitric oxide in the microcirculation, *Am. J. Physiol.* 274 (1998) H1705–H1714.
- [9] I. L. Megson, Nitric oxide donor drugs, *Drugs Fut.* 25 (7) (2000) 701–715.
- [10] M. Postema, A. van Wamel, C. T. Lancée, N. de Jong, Ultrasound-induced encapsulated microbubble phenomena, *Ultrasound Med. Biol.* 30 (6) (2004) 827–840.
- [11] Y. Taniyama, K. Tachibana, K. Hiraoka, T. Namba, K. Yamasaki, N. Hashiya, M. Aoki, T. Ogihara, K. Yasufumi, R. Morishita, Local delivery of plasmid DNA into rat carotid artery using ultrasound, *Circulation* 105 (2002) 1233–1239.
- [12] R. V. Shohet, S. Chen, Y. T. Zhou, Z. Wang, R. S. Meidell, R. H. Unger, P. A. Grayburn, Echocardiographic destruction of albumin microbubbles directs gene delivery to the myocardium, *Circulation* 101 (2000) 2554–2556.
- [13] M. J. Shortencarier, P. A. Dayton, S. H. Bloch, P. A. Schumann, T. O. Matsunaga, K. W. Ferrara, A method for radiation-force localized drug delivery using gas-filled lipospheres, *IEEE Trans. Ultrason., Ferroelect., Freq. Contr.* 51 (7) (2004) 822–831.
- [14] M. Postema, N. de Jong, G. Schmitz, A. van Wamel, Creating antibubbles with ultrasound, *Proc. IEEE Ultrason. Symp.* (2005) in press.
- [15] M. Postema, N. de Jong, G. Schmitz, Nonlinear behavior of ultrasound-insonified encapsulated microbubbles, in: *Nonlinear Acoustics*, 2005, p. in press.
- [16] L. D. Landau, E. M. Lifshitz, *Theory of Elasticity*, Butterworth-Heinemann, Oxford, 1986, 3rd ed.
- [17] N. de Jong, Acoustic properties of ultrasound contrast agents, Ph.D. thesis, Erasmus Universiteit Rotterdam (1993).
- [18] M. Postema, N. de Jong, G. Schmitz, The physics of nanoshelled microbubbles, *Biomed. Tech.* 50 (S1) (2005) 748–749.
- [19] M. Postema, A. Bouakaz, M. Versluis, N. de Jong, Ultrasound-induced gas release from contrast agent microbubbles, *IEEE Trans. Ultrason., Ferroelect., Freq. Contr.* 52 (6) (2005) 1035–1041.
- [20] A. Bouakaz, P. J. A. Frinking, N. de Jong, N. Bom, Noninvasive measurement of the hydrostatic pressure in a fluid-filled cavity based on the disappearance time of micrometer-sized free gas bubbles, *Ultrasound Med. Biol.* 25 (9) (1999) 1407–1415.

- [21] L. D. Landau, E. M. Lifshitz, Fluid Mechanics, Elsevier Butterworth-Heinemann, Oxford, 1987, 2nd ed.
- [22] M. Postema, A. Bouakaz, N. de Jong, Noninvasive microbubble-based pressure measurements: a simulation study, *Ultrasonics* 42 (1–9) (2004) 759–762.
- [23] M. Postema, A. van Wamel, F. J. ten Cate, N. de Jong, High-speed photography during ultrasound illustrates potential therapeutic applications of microbubbles, *Med. Phys.* 32 (12) (2005) 3707–3711.
- [24] J. R. Lancaster Jr., A tutorial on the diffusibility and reactivity of free nitric oxide, *Nitric Oxide: Biol. Chem.* 1 (1) (1997) 18–30.
- [25] E. Wilhelm, R. Battino, R. J. Wilcock, Low-pressure solubility of gases in liquid water, *Chem. Rev.* 77 (2) (1977) 219–262.

parameter	value	reference
$C_i/C_0$	0	
$D$ (37°C)	3300 $\mu\text{m}^2 \text{s}^{-1}$	[24, 4]
$L$ (35°C)	0.04202	[25]
$p_0$	1 atm	
$p_{\text{ov}}$	0 or 100 mmHg	
$\sigma$	0.055 $\text{N m}^{-1}$	

Table 1: Parameters for computation of NO dissolution.

## List of Figures

- 1 Schematic representation of a vessel cross-section, including an erythrocyte-free plasma layer. . . . 10
- 2 High-speed photograph of gas release from two stiff-shelled microbubbles during in an ultrasound field. The released gas has expanded due to the rarefaction phase of the ultrasound, whereas the the shells of the contrast agent microbubbles are too stiff to expand. The exposure time is 10 ns. The frame corresponds to a  $88 \times 58 \mu\text{m}^2$  area. . . . . 10
- 3 Diameter–time curves of dissolving NO gas bubbles at atmospheric pressure. . . . . 10
- 4 Acoustic amplitudes of dissolving air bubbles at 0, 60, 100, and 200 mmHg overpressure, respectively. . . . . 10
- 5 Acoustic amplitude after release as a function of overpressure applied, normalized by 1 mV. . . . 10

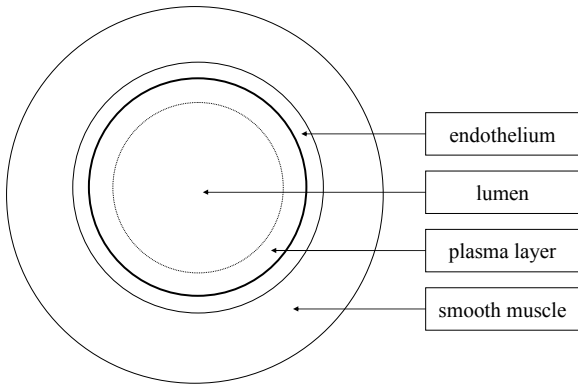


Figure 1: Schematic representation of a vessel cross-section, including an erythrocyte-free plasma layer.

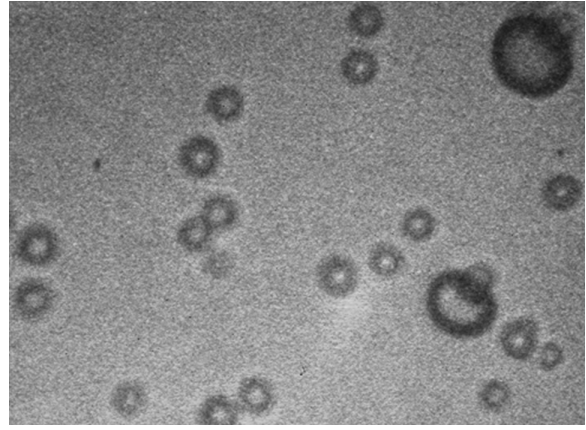


Figure 2: High-speed photograph of gas release from two stiff-shelled microbubbles during in an ultrasound field. The released gas has expanded due to the rarefaction phase of the ultrasound, whereas the the shells of the contrast agent microbubbles are too stiff to expand. The exposure time is 10 ns. The frame corresponds to a  $88 \times 58 \mu\text{m}^2$  area.

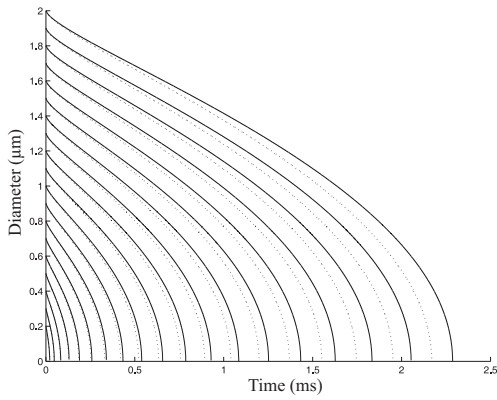


Figure 3: Diameter-time curves of dissolving NO gas bubbles at atmospheric pressure.

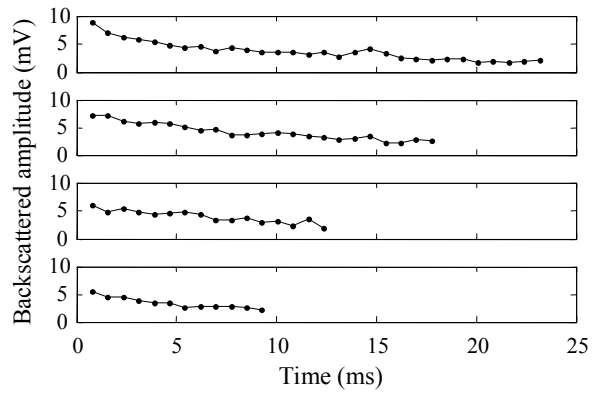


Figure 4: Acoustic amplitudes of dissolving air bubbles at 0, 60, 100, and 200 mmHg overpressure, respectively.

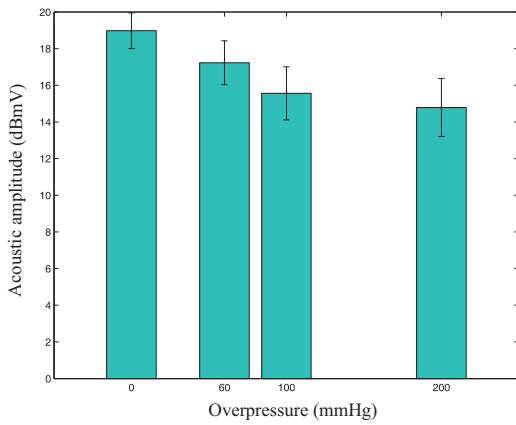


Figure 5: Acoustic amplitude after release as a function of overpressure applied, normalized by 1 mV.